Int. J. Solids Structures Vol. 29, No. 8, pp. 947–972, 1992
Printed in Great Britain.

0020–7683/92 $5.00 + .00

SLIGHTLY CURVED OR KINKED CRACKS IN ANISOTROPIC ELASTIC SOLIDS

HUAJIAN GAO and CHENG-HSIN CHIU
Division of Applied Mechanics, Stanford University, Stanford, CA 94305, U.S.A.

(*Received* 5 *February* 1991; *in revised form* 8 *August* 1991)

Abstract—Slightly curved or kinked cracks in anisotropic elastic solids are studied via a perturbation analysis valid for the second order accuracy in the deviation of the crack surfaces from a straight line. The analysis is based on complex variable representations in the Stroh formalism and known solutions for a perfectly straight reference crack. First and second order perturbation solutions are given for the stress intensity factors at the tip of a finite curved crack under remote stresses in a solid with arbitrary anisotropy, and are used to establish an approximate relationship between the apparent and local stress intensities at a crack tip, in view of the possible shielding effects of the crack surface morphology near the tip. The role of anisotropy is examined for a number of problems including circular arc cracks, slightly jogged or kinked cracks, cosine wavy cracks, etc. In several cases, further insight into the anisotropic effect on crack curving or kinking is provided by specializing the general perturbation formulae to cracks in materials with orthotropic symmetry. In the limiting case of a crack with an infinitesimal branch length, comparison with numerical results reported in the literature indicates that our perturbation solutions are accurate over the full range of practically important branch angles, up to nearly 150°.

For anisotropic elastic solids, various fracture criteria such as those based on energy release rate, G, and stress intensity factors, K_I and K_{II}, cease to give consistent predictions on crack behaviour. By investigating the effects of mode mixity, material anisotropy and non-singular T-stress on the behaviour of a nearly symmetric crack path in an orthotropic solid, we show that the K-based fracture criteria lead to very peculiar, perhaps even physically unreasonable, predictions such as: (i) branch angle at a mixed mode crack tip becomes infinite as the compliances perpendicular and parallel to the crack, S_{xx}/S_{yy}, reach a four-fold difference; (ii) the sign of the branch angle is reversed when $S_{xx}/S_{yy} > 4$, with the consequence of reversing the role of the non-singular T stress on the stability of a symmetric fracture path, namely, the path becomes stable for $T > 0$ and unstable for $T < 0$. Further, the mode I stress intensity factor, K_I, becomes a local minimum with respect to crack angle once $S_{xx}/S_{yy} > 4$. In contrast, the G-based criterion gives reasonable predictions such as: (i) cracks under mixed mode loading always tend to branch toward symmetric orientations; (ii) material and loading asymmetries play an equivalent role in affecting crack branching near a symmetric orientation; (iii) a compressive T stress always tends to stabilize a symmetric fracture path while a tensile T stress destabilizes such a path. For general crack path stability, the role of anisotropy can be manifested through (i) the value of T-stress at the crack tip and (ii) the variation of fracture resistance with respect to crack orientation.

INTRODUCTION

Curved or kinked cracks are frequently observed in the fracture of brittle materials under non-uniform loading or material conditions. For isotropic materials, the phenomenon of crack kinking, also referred to as branching, under mixed mode loading conditions has been the subject of extensive theoretical and experimental investigations [e.g. Erdogan and Sih (1963); Sih (1973); Hussain *et al.* (1974); Bilby and Cardew (1975); Lo (1978); Palaniswamy and Knauss (1978); Wu (1979a, b); Cotterell and Rice (1980); Karihaloo *et al.* (1981); Hayashi and Nemat-Nasser (1981); He and Hutchinson (1989)]. In addition to the usual singular integral equation approach by modelling the curved crack as a continuous distribution of dislocations, a convenient perturbation method based on Muskhelishvilli's complex variable representations has been developed (Banichuk, 1970; Goldstein and Salganik, 1970, 1974; Cotterell and Rice, 1980; Karihaloo *et al.*, 1981; Sumi *et al.*, 1983; Sumi, 1986) for two-dimensional curved cracks which do not deviate far from a straight line. The perturbation solutions, which approximately satisfy the boundary conditions along the crack surfaces, have been used to explain curved or branched crack extensions during quasi-static crack propagation. Cotterell and Rice (1980) used stress intensity factor solutions of first order accuracy to examine the stability of the fracture path of a quasi-statically growing crack under symmetric (mode I) loading conditions; they found that the path stability is controlled by the non-singular stress term T, acting in parallel with the

crack, in the Irwin–Williams expansion of the crack tip field: the symmetric path is found to be stable if $T < 0$ and unstable if $T > 0$. This stability criterion has since been widely used in explaining or predicting crack growth under various loading and material conditions. Karihaloo *et al.* (1981) carried out a second order perturbation analysis for two-dimensional curved cracks in isotropic materials and reached similar conclusions on issues such as the fracture path stability. The perturbation analysis has also been extended to curved crack growth in a finite two-dimensional isotropic body [e.g. Sumi *et al.* (1983); Sumi (1986)]. Most recently, Gao (1991a) has presented a perturbation analysis for three-dimensional slightly non-planar cracks using the Bueckner–Rice weight function method. In a three-dimensional configuration, assuming that a planar crack occupies the x_1–x_3 plane with normal in the x_2 direction and the crack front parallel to the x_3-axis, there exist three T-stress components, namely, T_{11}, T_{13} and T_{33}. Gao (1991a) found that, while the two-dimensional T-stress, T_{11}, plays a dominant role in controlling the stability of the crack against deflection in the fracture path in the x_1–x_2 plane, the other two T-components, T_{13} and T_{33}, control the stability of crack surfaces against non-planar perturbations parallel to the crack front. For example, a tensile T_{33} could give rise to a non-planar crack configuration in the form of en-echelon crack front segmentation.

With the advance of composite materials in recent years, it is of growing interest to understand the behaviour of cracks in anisotropic elastic solids. The problem of branched cracks under anisotropic material conditions has already received limited investigation (Miller and Stock, 1989; Obata *et al.*, 1989) using coupled singular integral equation approaches. Our paper is aimed at developing a two-dimensional perturbation analysis for examining the role of anisotropy on curved or kinked crack growth behaviours. We give perturbation solutions which are valid to the second order accuracy in the deviation of the crack surfaces from a straight line. Solutions in remarkably simple forms are derived for the stress intensity factors at the tip of a slightly curved crack. Applications of the perturbation results include studies of circular arc cracks, slightly jogged or branched cracks, cosine wavy crack surface profiles, etc. In several cases, our results are specialized to materials with orthotropic symmetry in order to provide further insight and better understanding of the role of anisotropy. The perturbation formulae also provide an approximate relationship between the apparent values and the crack-tip values for the stress intensity factors in view of the non-planarity in crack surface morphology near a crack tip. In the case of cracks with an infinitesimal branch length, comparison with existing numerical results reported by Obata *et al.* (1989) indicates that the perturbation solutions are, amazingly, accurate over the full range of practically important branch angle, up to nearly 150°.

It is known that various crack growth criteria, such as those based on maximum energy release rate, G, or maximum mode I stress intensity factor, K_I, or zero mode II, $K_{II} = 0$, give consistent predictions for crack behaviour in isotropic solids. However, in the anisotropic case, these fracture criteria cease to be consistent with one another. By investigating the effects of mode mixity, material anisotropy and T-stress on the behaviour of a nearly symmetric crack path in orthotropic solids, we show that the crack growth criteria based on maximum K_I or zero K_{II} lead to peculiar, perhaps even physically unreasonable, predictions. For example, the K-based criteria suggest that the branch angle at a mixed mode crack tip becomes infinite as the compliances perpendicular and parallel to the crack direction reach a four-fold ratio; the sign of the branch angle is also reversed across the same compliance ratio, with the consequence of also reversing the role of T-stress on the stability of a symmetric crack path, namely, the path becomes stable for $T > 0$ and unstable for $T < 0$, in contradiction to the common physical intuition. In contrast, there is no such peculiarity if the G-based crack growth criterion is used. The energy release rate along a symmetric crack path is found to be always a local maximum with respect to branch angle. The maximum G criterion also gives reasonable predictions such as: (i) mixed mode cracks always tend to branch toward symmetric orientations; (ii) material and loading asymmetries play an equivalent role in affecting crack branching near a symmetric orientation; (iii) a compressive T-stress always tends to stabilize a symmetric crack path while a tensile T-stress destabilizes such a path. For general crack path stability, the role of anisotropy can

be manifested by affecting (i) the value of T-stress at the crack tip and (ii) the variation of fracture resistance with respect to crack orientation. In addition, we have discovered an important error in Obata *et al.* (1989) which has previously resulted in some false conclusions on the behaviour of energy release rate with respect to crack branching in anisotropic elastic solids.

COMPLEX VARIABLE REPRESENTATIONS FOR ANISOTROPIC ELASTIC DEFORMATION

Stroh formalism

Our analysis will be based on the elegant anisotropic elasticity theory developed by Eshelby *et al.* (1953), Stroh (1958, 1962), Lekhnitskii (1963) and many others [e.g. Savin (1961); Barnett and Lothe (1973, 1974, 1985); Ingebrigtsen and Tonning (1969); Ting (1982); Suo (1990); Gao *et al.* (1991)] over the past nearly four decades. Previous applications have indicated that the stress analysis of an anisotropic body is often no more difficult than its isotropic counterpart, because the representation stress functions in the isotropic case are bi-harmonic while those in the seemingly more complex anisotropic problems are only harmonic-like functions. In the present literature on the anisotropic elasticity, there is unfortunately no single preferred notational system. To simplify the notations, we shall adopt a complex variable representation which is solely based on the concept of a surface admittance tensor to be described shortly.

With respect to a fixed Cartesian coordinate system x_i $(i = 1, 2, 3)$ an anisotropic elastic problem involves solution of the elastic equilibrium equation and the generalized Hooke's law:

$$\sigma_{ij} = C_{ijkl}u_{k,l}, \tag{1}$$

where σ_{ij} denotes the stress components, u_k are the displacements, C_{ijkl} is the fourth-order moduli tensor and comma means differentiation. For two-dimensional anisotropic problems in which the deformation field is independent of the x_3 coordinate, Stroh (1958, 1962) developed a powerful formalism which involves a six-dimensional eigenvalue equation

$$\mathbf{N}\xi = p\xi, \tag{2}$$

where ξ is a six-dimensional vector,

$$\xi^{\mathrm{T}} = (a_1, a_2, a_3, l_1, l_2, l_3) \tag{3}$$

and $\mathbf{N}$ is a real 6×6 matrix

$$\mathbf{N} = \begin{bmatrix} -\mathbf{T}^{-1}\mathbf{R}^{\mathrm{T}} & \mathbf{T}^{-1} \\ \mathbf{R}\mathbf{T}^{-1}\mathbf{R}^{\mathrm{T}} - \mathbf{Q} & -\mathbf{R}\mathbf{T}^{-1} \end{bmatrix}. \tag{4}$$

Bold letters are used here for vectors, tensors and matrices; the 3×3 matrices $\mathbf{T}$, $\mathbf{R}$, $\mathbf{Q}$ are related to the elastic moduli tensor C_{ijkl} as

$$(\mathbf{Q})_{ik} = C_{i1k1}, \quad (\mathbf{R})_{ik} = C_{i1k2}, \quad (\mathbf{T})_{ik} = C_{i2k2}. \tag{5}$$

The six eigenvalues p_α, which occur as three complex conjugate pairs, can be arranged so that the first three p_α have positive imaginary parts. Let two 3×3 matrices $\mathbf{A}$ and $\mathbf{L}$ have the components of the first three eigenvectors, $a_{i\alpha}$ and $l_{i\alpha}$, with both indices i and α ranging over 1, 2, 3. The surface impedance tensor $\mathbf{Z}$ and admittance tensor $\mathbf{Y}$ are then defined as

$$\mathbf{Z} = -i\mathbf{L}\mathbf{A}^{-1}, \quad \mathbf{Y} = \mathbf{Z}^{-1} = i\mathbf{A}\mathbf{L}^{-1}. \tag{6}$$

Both $\mathbf{Z}$ and $\mathbf{Y}$ are positive definite and hermitian, and obey the second order tensor

transformation rule under coordinate rotations in the x_1–x_2 plane (Barnett and Lothe, 1973; Ting, 1982). Barnett and Lothe (1985) have examined in sufficient detail the important properties of **Z** and **Y** in studying surface (Rayleigh) wave and interfacial (Stoneley) wave problems. The hermitian property

$$\mathbf{Z} = \bar{\mathbf{Z}}^{\mathrm{T}}, \quad \mathbf{Y} = \bar{\mathbf{Y}}^{\mathrm{T}} \tag{7}$$

indicates the real parts Re [**Z**], Re [**Y**] are symmetric real matrices while the imaginary parts Im [**Z**], Im [**Y**] are anti-symmetric real matrices.

To simplify the notation, we shall adopt an anisotropic operator (*) by the convention [also see, Gao (1991b); Gao *et al.* (1991)]:

$$\mathbf{q} * f(z; p) = \mathbf{L}\,\mathrm{diag}\,[f(z_1; p_1), f(z_2; p_2), f(z_3; p_3)]\mathbf{L}^{-1}\mathbf{q}, \tag{8}$$

where **q** is an arbitrary vector and the three Stroh eigenvalues p_α ($\alpha = 1, 2, 3$) form three complex variables $z_\alpha = x_1 + p_\alpha x_2$. The operator (*) incorporates the coupling of three Stroh eigenmodes such that a vector anisotropic complex potential function

$$\mathbf{\Phi}(z) = \mathbf{q} * f(z) \tag{9}$$

can be introduced to represent the displacement field **u** as

$$\mathbf{u} = \mathrm{Im}\,[\mathbf{Y}\mathbf{\Phi}(z)]. \tag{10}$$

The stress components σ_{kj}, which constitute two stress vectors

$$\mathbf{t}_1 = \begin{Bmatrix} \sigma_{11} \\ \sigma_{12} \\ \sigma_{13} \end{Bmatrix}, \quad \mathbf{t}_2 = \begin{Bmatrix} \sigma_{21} \\ \sigma_{22} \\ \sigma_{23} \end{Bmatrix}, \tag{11}$$

are given by

$$\mathbf{t}_1 = -\mathrm{Re}\,[\mathbf{\Phi}_{,2}(z)], \quad \mathbf{t}_2 = \mathrm{Re}\,[\mathbf{\Phi}_{,1}(z)]. \tag{12}$$

On an arbitrary curve in the x_1–x_2 plane having normal **n** and tangent **s**, it may be shown that the traction vector $\mathbf{t}_n$ [i.e. $(\mathbf{t}_n)_j = \sigma_{nj}$] and the hoop stress vector $\mathbf{t}_s$ [i.e. $(\mathbf{t}_s)_j = \sigma_{sj}$] are

$$\mathbf{t}_n = -\mathrm{Re}\,[\mathbf{\Phi}_{,s}(z)], \quad \mathbf{t}_s = \mathrm{Re}\,[\mathbf{\Phi}_{,n}(z)]. \tag{13}$$

Further, the resultant traction on an arc from point A to point B is

$$\mathbf{p} = \int_A^B \mathbf{t}_n\,\mathrm{d}s = \mathrm{Re}\,[\mathbf{\Phi}(A)] - \mathrm{Re}\,[\mathbf{\Phi}(B)]. \tag{14}$$

Stroh quantities for orthotropic materials

A special case of importance is an orthotropic material with three mutually orthogonal symmetry planes. The in-plane and out-of-plane deformation decouples if the coordinate plane x_1–x_2 coincides with one of the material symmetry planes. In that case, the Stroh matrix **L** for in-plane deformation becomes 2×2 as (Lekhnitskii, 1963):

$$\mathbf{L} = \begin{bmatrix} -p_1 & -p_2 \\ 1 & 1 \end{bmatrix}. \tag{15}$$

It suffices to consider the plane stress condition with 6×6 compliance matrix $s_{ij} = s_{ji}$, as

plane strain solutions can be obtained from plane stress solutions simply by replacing the compliance matrix as

$$s_{ij} - \frac{s_{i3}s_{j3}}{s_{33}} \to s_{ij}. \tag{16}$$

The Stroh eigenvalues for in-plane deformation, p_1, $\bar{p}_1$, p_2, $\bar{p}_2$, are solved from the fourth-order equation (Lekhnitskii, 1963):

$$s_{11}p^4 - 2s_{16}p^3 + (2s_{12}+s_{66})p^2 - 2s_{26}p + s_{22} = 0. \tag{17}$$

The surface admittance tensor is

$$\mathbf{Y} = \begin{bmatrix} s_{11}\,\mathrm{Im}\,(p_1+p_2) & -i(p_1p_2s_{11}-s_{12}) \\ i(\bar{p}_1\bar{p}_2s_{11}-s_{12}) & -s_{22}\,\mathrm{Im}\,(p_1^{-1}+p_2^{-1}) \end{bmatrix}. \tag{18}$$

The basic relation $p_1p_2\bar{p}_1\bar{p}_2 = s_{22}/s_{11}$ suggests that

$$\mathrm{Re}\,[\mathbf{Y}] = s_{11}\,\mathrm{Im}\begin{bmatrix} p_1+p_2 & \bar{p}_1\bar{p}_2 \\ \bar{p}_1\bar{p}_2 & -\bar{p}_1\bar{p}_2(p_1+p_2) \end{bmatrix}. \tag{19}$$

This matrix appears in the energy release rate expression for cracks in orthotropic solids.

For convenience we shall designate the orientations of material symmetry within the x_1–x_2 plane as x, or [100], and y, or [010]. Following the usual engineering convention [e.g. Tsai and Hahn (1980)], we shall write the four on-axis orthotropic constants by letter subscript, S_{xx}, S_{yy}, S_{xy} and S_{ss}, to distinguish them from numerical subscripts of the general off-axis orthotropic constants s_{ij}. The on-axis constants are sometimes written in terms of Young's moduli, shear moduli and Poisson ratio as (Tsai and Hahn, 1980):

$$S_{xx} = \frac{1}{E_x}, \quad S_{yy} = \frac{1}{E_y}, \quad S_{ss} = \frac{1}{E_s}, \quad S_{xy} = -\frac{\nu_x}{E_x} = -\frac{\nu_y}{E_y}. \tag{20}$$

When the coordinates x_1 and x_2 are coincident with the symmetry axes x and y, the Stroh eigenvalues (for in-plane deformation) satisfy the fourth-order equation

$$S_{xx}p^4 + (2S_{xy}+S_{ss})p^2 + S_{yy} = 0. \tag{21}$$

The two roots of (21) with positive imaginary parts satisfy

$$p_1^0p_2^0 = -\sqrt{S_{yy}/S_{xx}}, \quad p_1^0+p_2^0 = 2i\sqrt{\frac{\sqrt{S_{xx}S_{yy}}+S_{xy}+S_{ss}/2}{2S_{xx}}}. \tag{22}$$

In this case, eqn (19) reduces to

$$\mathrm{Re}\,[\mathbf{Y}^0] = S_{xx}\,\mathrm{Im}\,(p_1^0+p_2^0)\begin{bmatrix} 1 & 0 \\ 0 & \sqrt{S_{yy}/S_{xx}} \end{bmatrix}. \tag{23}$$

The off-axis quantities p_α, $\mathbf{Y}$ can be obtained from eqns (17) and (18), or alternatively from rotational transformations:

$$p_x(\theta) = \frac{p_x^0 \cos\theta - \sin\theta}{\cos\theta + p_x^0 \sin\theta} \tag{24}$$

$$\mathbf{Y}(\theta) = \mathbf{\Theta}\mathbf{Y}^0\mathbf{\Theta}^{\mathrm{T}}, \quad \mathbf{\Theta} = \begin{bmatrix} \cos\theta & \sin\theta \\ -\sin\theta & \cos\theta \end{bmatrix} \tag{25}$$

where θ denotes the angle between x_1 and the material axis x.

Further, for an arbitrary 2×1 vector $\mathbf{q}$,

$$\mathbf{q} * f(p) = \frac{1}{p_2 - p_1} \begin{bmatrix} p_2 f(p_2) - p_1 f(p_1) & p_1 p_2 [f(p_2) - f(p_1)] \\ -f(p_2) + f(p_1) & p_2 f(p_1) - p_1 f(p_2) \end{bmatrix} \begin{Bmatrix} q_1 \\ q_2 \end{Bmatrix}, \tag{26}$$

and in particular,

$$\mathbf{q} * p = \begin{bmatrix} p_1 + p_2 & p_1 p_2 \\ -1 & 0 \end{bmatrix} \begin{Bmatrix} q_1 \\ q_2 \end{Bmatrix} \tag{27}$$

$$\mathbf{q} * p^2 = \begin{bmatrix} p_1^2 + p_1 p_2 + p_2^2 & p_1 p_2 (p_1 + p_2) \\ -(p_1 + p_2) & -p_1 p_2 \end{bmatrix} \begin{Bmatrix} q_1 \\ q_2 \end{Bmatrix}. \tag{28}$$

In the isotropic limit, both eigenvalues p_1 and p_2 approach the complex unit i and eqn (26) becomes

$$\mathbf{q} * f(p) = \frac{\partial}{\partial p} \begin{bmatrix} pf(p) & -f(p) \\ -f(p) & f(p)/p \end{bmatrix}_{p=i} \begin{Bmatrix} q_1 \\ q_2 \end{Bmatrix}. \tag{29}$$

This relation is very useful for specializing orthotropic elastic solutions in the isotropic case.

SLIGHTLY CURVED FINITE CRACKS

Solution for a straight crack

The perturbation analysis for slightly curved cracks will be based on the reference solution for a perfectly straight crack. The solution for a straight crack subjected to remote stresses $\mathbf{t}_1^{\infty}$ and $\mathbf{t}_2^{\infty}$ is

$$\mathbf{\Phi}_0(z) = \mathbf{t}_2^{\infty} * \sqrt{z^2 - a^2} - \mathbf{t}_1^{\infty} x_2 \tag{30}$$

where

$$\mathbf{t}_{\mathrm{T}} = \mathbf{t}_1^{\infty} + \mathrm{Re}\,[\mathbf{t}_2^{\infty} * p] \tag{31}$$

represents the non-singular T-stress vector in the expansion of the crack tip field, which will play an important role in the perturbation analysis. Note that $\mathbf{t}_{\mathrm{T}}$ is related to both the stress $\mathbf{t}_1^{\infty}$ applied parallel to the crack and $\mathbf{t}_2^{\infty}$ normal to the crack. For a crack lying along the material axis x in an orthotropic solid subject to in-plane loading, one may use (27) and (22) to show that

$$\mathbf{t}_{\mathrm{T}} = \begin{bmatrix} T \\ 0 \end{bmatrix}, \quad \text{where} \quad T = \sigma_{11}^{\infty} - \sigma_{22}^{\infty} \sqrt{\frac{S_{yy}}{S_{xx}}}. \tag{32}$$

Thus, the T-stress can be significantly affected by the material anisotropy. Clearly, T in eqn (32) is always compressive under uniaxial tension, $\sigma_{22}^{\infty} > 0$ and $\sigma_{11}^{\infty} = 0$. In that case, the

magnitude of T increases with stiffness parallel to the crack and decreases with that perpendicular to the crack. Thus, cracks parallel to the stiffer material axis are subjected to more compressive T-stress than those along the weaker material axis under comparable stress state. For typical fiber reinforced composite materials, the ratio S_{yy}/S_{xx} can be as large as $10 \sim 30$, so that cracks parallel to fibers will be subjected to much more compressive T-stress compared to those perpendicular to fibers.

Following the solution in eqn (30) and the representations in eqns (10–12), the stress intensity factor $\mathbf{k}^{\infty}$ at the crack tip is

$$\mathbf{k}^{\infty} = \mathbf{t}_2^{\infty}\sqrt{\pi a} \tag{33}$$

and the traction at a distance r ahead of the crack tip is asymptotically given by

$$\begin{aligned} \mathbf{t}_1 &= \mathbf{t}_r - \mathrm{Re}\,[\mathbf{k}^{\infty} * p]\frac{1}{\sqrt{2\pi r}} + 0(\sqrt{r}) \\ \mathbf{t}_2 &= \frac{\mathbf{k}^{\infty}}{\sqrt{2\pi r}} + 0(\sqrt{r}). \end{aligned} \tag{34}$$

The above results will be used as the reference solutions in the perturbation analysis to follow.

Observe that the stress intensity factors at the above slit-like crack under remote stress are independent of material constants. Under uniaxial tension loading, the stress intensity factor solution is $K_I^c = \sigma_{22}^{\infty}\sqrt{\pi a}$ ($K_{II}^c = 0$). Since the crack is often considered as a degenerated elliptical hole, it would be interesting to compare the crack tip stress intensity factor with the stress concentration at an elliptical hole boundary having aspect ratio $a/b \gg 1$. For comparison, let the elliptical hole be aligned with the material axes and subjected to uniaxial tension σ_{22}^{∞}. The maximum hoop stress occurs at the semi-long axis, $x_1 = a$, with the value [e.g. Savin (1961)]:

$$\sigma_{\max} = \sigma_{22}^{\infty}\left\{1 + \frac{2a}{b}f\right\} \simeq \frac{2\sigma_{22}^{\infty}\sqrt{\pi a}}{\sqrt{\pi\rho}}f \tag{35}$$

where

$$f = \sqrt{\frac{\sqrt{S_{xx}S_{yy}} + S_{xy} + S_{ss}/2}{2S_{xx}}} \tag{36}$$

and $\rho = b^2/a$ denotes the local curvature. Curiously, the stress concentration factor for an elliptical hole does depend on material constants. In other words, elliptical holes with the same aspect ratio and loading but in different materials will have different stress concentration factors. This is in contrast to the stress intensity factor, as the measure of stress concentration at a sharp crack tip, which is completely independent of the material constants. The moduli coefficient f in eqns (35), (36) is equal to one for isotropic materials and can be as large as 2 or 3 for fiber reinforced composite materials.

Second order perturbation analysis

Consider a slightly curved crack along a curve $\tilde{c}$ with $\tilde{c}^+$ denoting the upper crack face and $\tilde{c}^-$ denoting the lower crack face. When the shape of $\tilde{c}$ is only slightly different from a straight line c, say along the x_1-axis over $-a < x_1 < a$, one may devise a perturbation

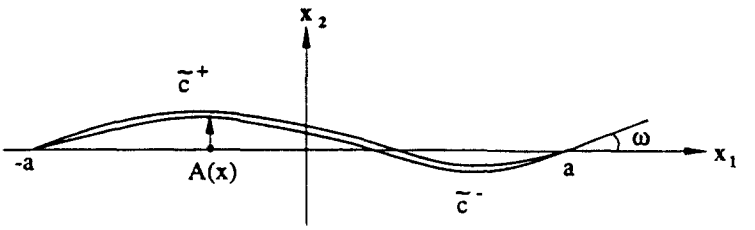

Fig. 1. Slightly curved crack configuration.

procedure to calculate solutions for the curved crack based on the solution $\Phi_0(z)$ for a reference straight crack. Let the curve $\tilde{c}$ be described by a function (Fig. 1):

$$x_2 = A(x_1) \tag{37}$$

over $-a < x_1 < a$, where $A(x_1)$ represents a small perturbation of the crack from its reference straight position (along the x_1-axis) to the actual curved position. The solution to the curved crack can be written in the perturbation form

$$\Phi(z) = \Phi_0(z) + \Phi_1(z) + \Phi_2(z) + \cdots \tag{38}$$

where $\Phi_1(z)$ and $\Phi_2(z)$ are, respectively, the first and second order "disturbance" terms. As a crack face point $\tilde{z}$ along $\tilde{c}^+$ or $\tilde{c}^-$ is perturbed to the corresponding reference position $(x, 0^+)$ or $(x, 0^-)$ along the reference crack, $\Phi(\tilde{z})$ is perturbed as

$$\Phi(\tilde{z}) = \Phi_0(x) + A(x)\Phi_{0,2}(x) + \frac{A^2(x)}{2}\Phi_{0,22}(x) + \Phi_1(x) + A(x)\Phi_{1,2}(x) + \Phi_2(x) \tag{39}$$

within second order accuracy. Letting the reference crack surfaces $c^\pm$ be subjected to the same traction as those on the curved crack surfaces $\tilde{c}^\pm$, the zeroth order equation is then obtained as

$$\mathrm{Re}\,[\Phi_0(x)] = \mathrm{Re}\,[\Phi(\tilde{z})] = -\mathbf{p} \quad \text{on } c^\pm \tag{40}$$

where $\mathbf{p}$ represents the resultant traction on an arc from a fixed point to the point $\tilde{z}$ moving along the crack surfaces. Taking the real part of eqn (39), then collecting the first and second order like terms leads to two boundary value equations:

$$\mathrm{Re}\,[\Phi_1(x)] = -A(x)\,\mathrm{Re}\,[\Phi_{0,2}(x)] \quad \text{on } c^\pm \tag{41}$$

and

$$\mathrm{Re}\,[\Phi_2(x)] = -\frac{A^2(x)}{2}\Phi_{0,22}(x) - A(x)\Phi_{1,2}(x) \quad \text{on } c^\pm \tag{42}$$

for determining the unknown functions $\Phi_1(x)$ and $\Phi_2(x)$. Equations (41) and (42) have converted the original curved crack problem to one involving an "effective" traction along the surfaces of the reference straight crack.

Now consider the case of remote stresses $\mathbf{t}_1^\infty$ and $\mathbf{t}_2^\infty$. The reference solution $\Phi^0(z)$ given in eqn (30) has boundary values $(\Phi_0)^\pm$ on the upper and lower crack surfaces which satisfy

$$(\Phi_{0,2})^+ + (\Phi_{0,2})^- = -2\mathbf{t}_T, \quad (\Phi_{0,22})^+ + (\Phi_{0,22})^- = 0. \tag{43}$$

Summing up the two boundary conditions in (41), one for the upper crack face (c^+) and one for the lower crack face (c^-), and then differentiating with respect to x_1 lead to

$$[\Phi_{1,1}(x) + \bar{\Phi}_{1,1}(x)]^+ + [\Phi_{1,1}(x) + \bar{\Phi}_{1,1}(x)]^- = 4\mathbf{t}_T A'(x). \tag{44}$$

The above Hilbert equation has the solution:

$$\Phi_{1,1}(z) + \bar{\Phi}_{1,1}(z) = -\frac{2}{\pi}\int_{-a}^{a} \mathbf{t}_T * \left(\frac{A'(\xi)\sqrt{a^2-\xi^2}}{(z-\xi)\sqrt{z^2-a^2}}\mathrm{d}\xi\right). \tag{45}$$

In particular, ahead of the crack tip ($|x| > a$), one may show that

$$\begin{aligned} \mathrm{Re}\,[\Phi_{1,1}(x)] &= -\frac{\mathbf{t}_T}{\pi}\int_{-a}^{a} \frac{A'(\xi)\sqrt{a^2-\xi^2}}{(x-\xi)\sqrt{x^2-a^2}}\mathrm{d}\xi \\ \mathrm{Re}\,[\Phi_{1,2}(x)] &= -\frac{\mathrm{Re}\,[\mathbf{t}_T * p]}{\pi}\int_{-a}^{a} \frac{A'(\xi)\sqrt{a^2-\xi^2}}{(x-\xi)\sqrt{x^2-a^2}}\mathrm{d}\xi. \end{aligned} \tag{46}$$

The first order solution (45) also satisfies the crack face condition

$$[\Phi_{1,2}(x) + \bar{\Phi}_{1,2}(x)]^+ + [\Phi_{1,2}(x) + \bar{\Phi}_{1,2}(x)]^- = 4(\mathbf{t}_T * p)A'(x). \tag{47}$$

Similar steps can be used to derive the second order solutions. Using the results in eqns (43) and (47), one can show that the boundary conditions given in (42) lead to the following Hilbert equation:

$$[\Phi_{2,1}(x) + \bar{\Phi}_{2,1}(x)]^+ + [\Phi_{2,1}(x) + \bar{\Phi}_{2,1}(x)]^- = -4(\mathbf{t}_T * p)[A'^2(x) + A(x)A''(x)]. \tag{48}$$

The solution to (48) is

$$\Phi_{2,1}(z) + \bar{\Phi}_{2,1}(z) = \frac{2}{\pi}\int_{-a}^{a} \mathbf{t}_T * \left(\frac{p[A'^2(\xi) + A(\xi)A''(\xi)]\sqrt{a^2-\xi^2}}{(z-\xi)\sqrt{z^2-a^2}}\mathrm{d}\xi\right). \tag{49}$$

Ahead of the crack tip ($|x| > a$), the second order solution gives

$$\mathrm{Re}\,[\Phi_{2,1}(x)] = \frac{\mathrm{Re}\,[\mathbf{t}_T * p]}{\pi}\int_{-a}^{a} \frac{[A'^2(\xi) + A(\xi)A''(\xi)]\sqrt{a^2-\xi^2}}{(x-\xi)\sqrt{x^2-a^2}}\mathrm{d}\xi. \tag{50}$$

As will be shown below, the perturbation results in eqns (46) and (50) are sufficient for determining the second-order-accurate perturbation solutions for the stress intensity factors.

At the right tip $x_1 = a$ of the curved crack, the stress intensity factors are defined such that the traction along the polar plane $\omega = A'(a)$, representing the prospective cracking line, is asymptotically given by

$$\Omega\mathbf{t}_\omega = \mathbf{k}/\sqrt{2\pi r} \tag{51}$$

where, by eqn (13),

$$\mathbf{t}_\omega = \mathrm{Re}\,[\Phi_r(z)] = \mathrm{Re}\,[\Phi_{0,r}(z) + \Phi_{1,1}(x) + \sin\omega\Phi_{1,2}(x) + \Phi_{2,1}(x)] \tag{52}$$

within the required second order accuracy. The rotation matrix

$$\mathbf{\Omega} = \begin{bmatrix} \cos\omega & \sin\omega & 0 \\ -\sin\omega & \cos\omega & 0 \\ 0 & 0 & 1 \end{bmatrix} \tag{53}$$

transforms the traction components in the Cartesian directions (x_1, x_2) to those in the polar directions (r, ω). Substituting (30), (46) and (50) into (52) and then using (51) lead to the final solution for the stress intensity factor $\mathbf{k}$ which is accurate to the second order in the deviation of the crack surfaces from a straight line. The result is

$$\mathbf{k} = \mathbf{\Omega}\left\{\mathrm{Re}\left[\mathbf{t}_2^{\infty} * \sqrt{\cos\omega + p\sin\omega}\right] - \frac{\mathbf{t}_T + \sin\omega\,\mathrm{Re}\left[\mathbf{t}_T * p\right]}{\pi a}\int_{-a}^{a} A'(\xi)\sqrt{\frac{a+\xi}{a-\xi}}\,\mathrm{d}\xi \right.$$
$$\left. + \frac{\mathrm{Re}\left[\mathbf{t}_T * p\right]}{\pi a}\int_{-a}^{a}\left[A'^2(\xi) + A(\xi)A''(\xi)\right]\sqrt{\frac{a+\xi}{a-\xi}}\,\mathrm{d}\xi\right\}\sqrt{\pi a}. \tag{54}$$

The first term within the curly brace in eqn (54) represents the geometric effect of the crack tip being tilted relative to the reference straight orientation. The second and third terms are due to the overall perturbation in crack shape. For an infinitesimal kink or branch at the tip of a pre-existing straight crack, the second and third terms vanish and the first term gives the second order accurate solutions for the stress intensity factors for the infinitesimal kink.

In most cases, with a few exceptions such as when studying the variation of the crack tip energy release rate (as will be considered later), it is often sufficient to examine the first order perturbation solutions. Within the first order accuracy, eqn (54) reduces to

$$\mathbf{k} = \left\{\mathbf{\Omega}\mathbf{t}_2^{\infty} + \frac{\omega}{2}\mathrm{Re}\left[\mathbf{t}_2^{\infty} * p\right] - \frac{\mathbf{t}_T}{\pi a}\int_{-a}^{a} A'(\xi)\sqrt{\frac{a+\xi}{a-\xi}}\,\mathrm{d}\xi\right\}\sqrt{\pi a} \tag{55}$$

where the first order expansion of $\mathbf{\Omega}$ is

$$\mathbf{\Omega} = \begin{bmatrix} 1 & \omega & 0 \\ -\omega & 1 & 0 \\ 0 & 0 & 1 \end{bmatrix}. \tag{56}$$

The explicit effect of material anisotropy shows up only in the second term within the curly brace. However, the T-stress vector $\mathbf{t}_T$ appearing in the third term is also affected by the anisotropy via eqn (31). To provide further insight into the anisotropic effects, consider the in-plane modes (I and II) of a crack lying along a symmetry plane in an orthotropic solid. Using eqns (22) and (27), the first order perturbation formulae can be recast into a more explicit form

$$K_{\mathrm{I}} = \left\{\sigma_{22}^{\infty} - \frac{3\omega}{2}\sigma_{21}^{\infty}\right\}\sqrt{\pi a}$$

$$K_{\mathrm{II}} = \left\{\sigma_{21}^{\infty} + \omega\sigma_{22}^{\infty}\left(1 - \frac{1}{2}\sqrt{\frac{S_{yy}}{S_{xx}}}\right)\right.$$
$$\left. - \frac{1}{\pi a}\left(\sigma_{11}^{\infty} - \sigma_{22}^{\infty}\sqrt{\frac{S_{yy}}{S_{xx}}}\right)\int_{-a}^{a} A'(\xi)\sqrt{\frac{a+\xi}{a-\xi}}\,\mathrm{d}\xi\right\}\sqrt{\pi a}. \tag{57}$$

Thus, within the first order accuracy, the mode I stress intensity factor is independent of the material anisotropy and, among the four on-axis orthotropic moduli (S_{xx}, S_{yy}, S_{xy}, S_{ss}), only S_{yy}/S_{xx}, the ratio of the stiffnesses perpendicular and parallel to the reference crack,

affects the mode II stress intensity. For materials with cubic symmetry, $S_{yy} = S_{xx}$ and the corresponding perturbation solutions become identical to those in isotropic solids.

It is worth pointing out that the perturbation solutions in (55) and (57) are consistent with the corresponding isotropic solutions in the literature [e.g. Cotterell and Rice (1980)] in which case

$$K_{\mathrm{I}} = \left\{\sigma_{22}^{\infty} - \frac{3\omega}{2}\sigma_{21}^{\infty}\right\}\sqrt{\pi a}$$

$$K_{\mathrm{II}} = \left\{\sigma_{21}^{\infty} + \frac{\omega}{2}\sigma_{22}^{\infty} - \frac{\sigma_{11}^{\infty} - \sigma_{22}^{\infty}}{\pi a}\int_{-a}^{a} A'(\xi)\sqrt{\frac{a+\xi}{a-\xi}}\,\mathrm{d}\xi\right\}\sqrt{\pi a}. \tag{58}$$

CIRCULAR ARC CRACK

For the circular arc crack geometry shown in Fig. 2, it can be shown that the integral in the first order perturbation formula (55) reduces to

$$\int_{-a}^{a} A'(\xi)\sqrt{\frac{a+\xi}{a-\xi}}\,\mathrm{d}\xi = \frac{\pi\omega a}{2}. \tag{59}$$

Substituting the above result into eqn (55) and then using eqn (31) for the T-stress vector $\mathbf{t}_T$, one finds

$$\mathbf{k} = \left\{\boldsymbol{\Omega}\mathbf{t}_2^{\infty} - \frac{\omega}{2}\mathbf{t}_1^{\infty}\right\}\sqrt{\pi a}. \tag{60}$$

This result shows that, within the first order accuracy, the stress intensity factors of a circular arc crack under remote stresses are independent of material anisotropy. In the component form, the first order solutions given in (60) are

$$K_{\mathrm{I}} = \sqrt{\pi a}\left(\sigma_{22}^{\infty} - \frac{3\omega}{2}\sigma_{12}^{\infty}\right)$$

$$K_{\mathrm{II}} = \sqrt{\pi a}\left[\sigma_{21}^{\infty} + \left(\sigma_{22}^{\infty} - \frac{\sigma_{11}^{\infty}}{2}\right)\omega\right]$$

$$K_{\mathrm{III}} = \sqrt{\pi a}\left(\sigma_{23}^{\infty} - \frac{\omega}{2}\sigma_{13}^{\infty}\right). \tag{61}$$

Cotterell and Rice (1980) have used existing analytical solutions for the circular arc crack in an isotropic solid to check the accuracy of eqns (61); they found that the mode I stress

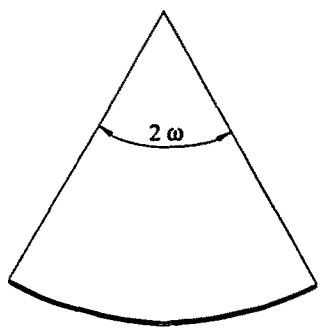

Fig. 2. A circular arc crack.

intensity factor result is accurate within 5% for $\omega < 15^\circ$ while the mode II result is accurate within 5% for $\omega < 40^\circ$. The analytical solution to circular arc cracks in anisotropic solids does not seem to exist yet. However, we expect that eqns (61) are of similar accuracy for the anisotropic cases. The second order solutions can be similarly obtained from eqn (54), but we are not pursuing that course here.

A JOGGED CRACK CONFIGURATION

Figure 3 shows a crack with a jog of magnitude A at distance l from the right crack tip. Such a fracture pattern frequently occurs in fiber reinforced composite materials. For this configuration, the first order eqn (55) yields,

$$\mathbf{k} = \left\{\mathbf{t}_2^\infty + \frac{\mathbf{t}_T A}{\pi a}\sqrt{\frac{2a-l}{l}}\right\}\sqrt{\pi a}. \tag{62}$$

Thus, for such a crack configuration, the effect of anisotropy is fully contained in the T-stress vector $\mathbf{t}_T$. Since $\mathbf{t}_T$ is parallel to the crack plane, the mode I stress intensity factor remains the same regardless of the jog and anisotropy. However, the mode II intensity factor depends on both the jog geometry and the anisotropy (through T-stress). In the orthotropic case, we find

$$K_{II} = \left\{\sigma_{21}^\infty + \frac{A}{\pi a}\left(\sigma_{11}^\infty - \sigma_{22}^\infty\sqrt{\frac{S_{yy}}{S_{xx}}}\right)\sqrt{\frac{2a-l}{l}}\right\}\sqrt{\pi a}. \tag{63}$$

For this solution to be valid, one should assume the conditions are such that the crack faces do not come into contact.

APPARENT VERSUS LOCAL STRESS INTENSITY FACTORS FOR SLIGHTLY CURVED CRACKS

"Apparent" crack-tip field

As a more basic configuration, consider a semi-infinite straight crack with a given stress intensity factor $\mathbf{k}^\infty$ and a given T-stress vector $\mathbf{t}_T$. The solution can be written as

$$\Phi^0(z) = \frac{1}{\pi}\mathbf{k}^\infty * \sqrt{2\pi z} - \mathbf{t}_T x_2. \tag{64}$$

A fundamental problem can be posed as follows. The value of $\mathbf{k}^\infty$, calculated by assuming that the crack is perfectly straight without accounting for the detailed morphological microstructure along the crack faces, represents the "apparent" stress intensity factors for the cracked body. Since the actual crack surfaces may not be perfectly flat, rather they may exhibit some non-planarity due to inhomogeneities on the microscale, the "real" stress intensity factor $\mathbf{k}$ acting at the crack tip will differ from its apparent value $\mathbf{k}^\infty$. The questions are how to determine $\mathbf{k}$ from $\mathbf{k}^\infty$, and how the non-planar crack surface morphology, i.e. curving or kinking, combined with material anisotropy, affects the crack growth which is

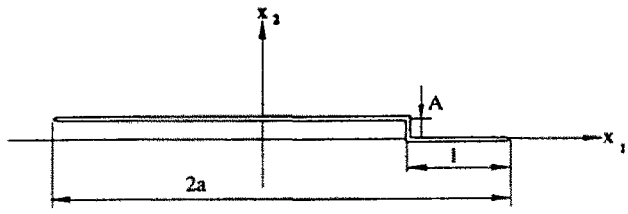

Fig. 3. A jogged crack configuration.

governed by the local stress intensity **k**, rather than $\mathbf{k}^{\infty}$. The perturbation analysis can provide some approximate description and understanding on these issues.

Apparent $\mathbf{k}^{\infty}$ *versus local* **k**

The relation between the apparent stress intensity factor $\mathbf{k}^{\infty}$ and the local crack tip value **k** can be obtained from the perturbation formulae derived in the last section. Letting the size of the crack approach infinity in the finite crack formula (54), one finds the second order formula

$$\mathbf{k} = \boldsymbol{\Omega}\,\mathrm{Re}\,[\mathbf{k}^{\infty} * \sqrt{\cos\omega + p\sin\omega}] - (\mathbf{t}_T + \sin\omega\,\mathrm{Re}\,[\mathbf{t}_T * p])\sqrt{\frac{2}{\pi}}\int_{-\infty}^{0}\frac{A'(\xi)\,\mathrm{d}\xi}{\sqrt{-\xi}} + \mathrm{Re}\,[\mathbf{t}_T * p]\sqrt{\frac{2}{\pi}}\int_{-\infty}^{0}\frac{A'^2(\xi) + A(\xi)A''(\xi)}{\sqrt{-\xi}}\,\mathrm{d}\xi, \quad (65)$$

where ω, again, is the local tangent at the crack tip. Once the crack surface profile $A(\xi)$ and the T-stress vector $\mathbf{t}_T$ are given, the above equation can be immediately used to calculate the crack tip stress intensity factor **k** from the apparent value $\mathbf{k}^{\infty}$. Often it may be sufficient to examine the first order result

$$\mathbf{k} = \boldsymbol{\Omega}\mathbf{k}^{\infty} + \frac{\omega}{2}\,\mathrm{Re}\,[\mathbf{k}^{\infty} * p] - \mathbf{t}_T\sqrt{\frac{2}{\pi}}\int_{-\infty}^{0}\frac{A'(\xi)\,\mathrm{d}\xi}{\sqrt{-\xi}}. \quad (66)$$

For orthotropic solids cracked along a symmetry axis, the first order formulae become

$$K_{\mathrm{I}} = K_{\mathrm{I}}^{\infty} - \frac{3\omega}{2}K_{\mathrm{II}}^{\infty}$$

$$K_{\mathrm{II}} = K_{\mathrm{II}}^{\infty} + \omega K_{\mathrm{I}}^{\infty}\left(1 - \frac{1}{2}\sqrt{\frac{S_{yy}}{S_{xx}}}\right) - T\sqrt{\frac{2}{\pi}}\int_{-\infty}^{0}\frac{A'(\xi)\,\mathrm{d}\xi}{\sqrt{-\xi}}. \quad (67)$$

Cosine wavy crack surfaces

Suppose that the crack surface is of a wavy profile given by (Fig. 4):

$$A(x_1) = A\cos\frac{2\pi(x_1 - l)}{\lambda} \quad (68)$$

where A is the wave amplitude and λ is the wavelength. The aspect ratio A/λ characterizes the "roughness" of the crack surface morphology. Substituting (68) into (66) yields

$$\mathbf{k} = \boldsymbol{\Omega}\mathbf{k}^{\infty} + \frac{\omega}{2}\,\mathrm{Re}\,[\mathbf{k}^{\infty} * p] - 2A\mathbf{t}_T\sqrt{\frac{\pi}{\lambda}}\sin\left(\frac{2\pi l}{\lambda} + \frac{\pi}{4}\right). \quad (69)$$

Here $\omega = A'(0) = (2\pi A/\lambda)\sin 2\pi l/\lambda$. Thus, the effect of a wavy crack surface increases with the surface roughness. For such a crack lying along an orthotropic axis, letting $l = 0$ so that the crack tip is at the wave peak, we find

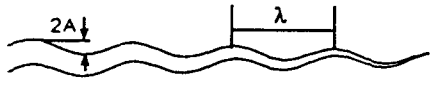

Fig. 4. Cosine wavy crack profile.

$$K_{\mathrm{I}} = K_{\mathrm{I}}^{x}, \quad K_{\mathrm{II}} = K_{\mathrm{II}}^{x} - TA\sqrt{\frac{2\pi}{\lambda}}. \tag{70}$$

In this case, the wavy crack surface does not affect the mode I stress intensity factor K_{I} (within first order accuracy), but can have a significant effect on K_{II}, especially when the crack surfaces have a rough morphology.

KINKED CRACKS

When a straight crack is loaded asymmetrically or encounters a weak plane with lower fracture toughness, the new crack initiates at an angle to the old one. This phenomenon of crack kinking or branching has been studied extensively in the past literature. In particular, branched cracks in anisotropic materials have been investigated numerically via coupled singular integral equations by Miller and Stock (1989) and Obata *et al.* (1989). In comparison, our perturbation analysis provides more explicit formulae to examine the crack branching in materials with arbitrary anisotropy.

Assume that a finite crack undergoes a branched extension of length l at the right tip, as shown in Fig. 5a. In this case, the overall projection length of the crack on the x_1 axis is $2a$. Perturbation solutions accurate up to second order in ω could be immediately obtained from eqns (54) and (55). For example, application of the first order formula (55) results in

$$\mathbf{k} = \left\{\boldsymbol{\Omega}\mathbf{t}_2^{\zeta} + \frac{\omega}{2}\mathrm{Re}\left[\mathbf{t}_2^{\zeta} * p\right] - \frac{\omega \mathbf{t}_r}{\pi}\left(\cos^{-1}\frac{a_0}{a} + \sqrt{1-\frac{a_0^2}{a^2}}\right)\right\}\sqrt{\pi a} \tag{71}$$

for the single kink in Fig. 5a and

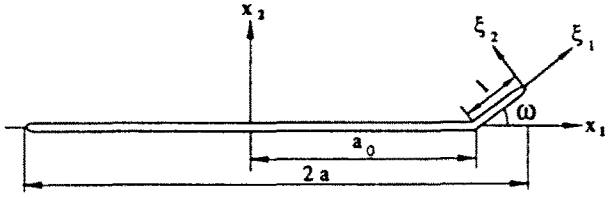

(a)

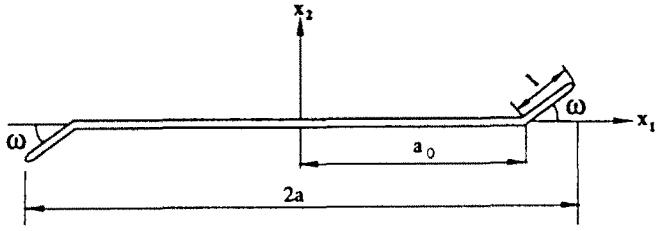

(b)

Fig. 5. Kinked crack configurations.

$$\mathbf{k} = \left\{\Omega \mathbf{t}_2^{\infty} + \frac{\omega}{2}\,\mathrm{Re}\,[\mathbf{t}_2^{\infty} * p] - \frac{2\omega \mathbf{t}_T}{\pi}\cos^{-1}\frac{a_0}{a}\right\}\sqrt{\pi a} \tag{72}$$

for the double-kink in Fig. 5b. Here the length parameter a_0 is given by

$$a_0 = a - l\cos\omega. \tag{73}$$

These solutions become more explicit for the orthotropic material cases. For a double-kinked crack with main crack along the material axis x,

$$K_{\mathrm{I}} = \sqrt{\pi a}\left(\sigma_{22}^{\infty} - \frac{3\omega}{2}\sigma_{11}^{\infty}\right)$$

$$K_{\mathrm{II}} = \sqrt{\pi a}\left[\sigma_{21}^{\infty} + \omega\sigma_{22}^{\infty}\left(1 - \frac{1}{2}\sqrt{\frac{S_{yy}}{S_{xx}}}\right) - \frac{2\omega}{\pi}\cos^{-1}\frac{a_0}{a}\left(\sigma_{11}^{\infty} - \sigma_{22}^{\infty}\sqrt{\frac{S_{yy}}{S_{xx}}}\right)\right]. \tag{74}$$

One can also obtain the second order perturbation solutions from eqn (54), if desired.

Once a kink, representing a small deviation from the main crack path, is established at the tip of a growing crack, the crack opens so that the displacements near the tip are proportional to the square root of the distance from the tip and the energy release rate is given by [e.g. Barnett and Asaro (1972)]:

$$G = \tfrac{1}{2}\mathbf{k}^{\mathrm{T}}\,\mathrm{Re}\,[\mathbf{Y}']\mathbf{k}. \tag{75}$$

This relation, together with the perturbation solutions for $\mathbf{k}$, can be used to examine the behavior of energy release rate at crack branching. Primed quantities such as $\mathbf{Y}'$ in eqn (75) are associated with the crack tip local coordinates ξ_1, ξ_2 (Fig. 5a). In the orthotropic case, use of eqn (19) leads to

$$G = \tfrac{1}{2}s'_{11}\,\mathrm{Im}\,[K_{\mathrm{II}}^2(p'_1 + p'_2) + 2K_{\mathrm{I}}K_{\mathrm{II}}\bar{p}'_1\bar{p}'_2 - K_{\mathrm{I}}^2(p'_1 + p'_2)\bar{p}'_1\bar{p}'_2]. \tag{76}$$

This expression was first derived by Sih *et al.* (1965).

A special case of particular interest is an infinitesimal kink at the crack tip. In that case, the perturbation formula in eqn (54) suggests that the solution

$$\mathbf{k} = \boldsymbol{\Omega}\,\mathrm{Re}\,[\mathbf{t}_2^{\infty} * \sqrt{\cos\omega + p\sin\omega}]\sqrt{\pi a} \tag{77}$$

is accurate to second order in the kink angle ω. For orthotropic solids, let θ denote the angle between the reference crack coordinates (x_1, x_2) and the material coordinates (x, y). Then the crack tip local coordinates (ξ_1, ξ_2) are connected to (x, y) by two consecutive rotations, $\boldsymbol{\Theta}$ and $\boldsymbol{\Omega}$. According to tensor transformation law,

$$\mathbf{Y}' = \boldsymbol{\Omega}\boldsymbol{\Theta}\mathbf{Y}^0\boldsymbol{\Theta}^{\mathrm{T}}\boldsymbol{\Omega}^{\mathrm{T}} \tag{78}$$

where $\mathbf{Y}^0$ refers to the material coordinates (x, y) and the rotation matrices $\boldsymbol{\Theta}$ and $\boldsymbol{\Omega}$ have been defined in eqns (25) and (53). (For orthotropic symmetry, $\boldsymbol{\Omega}$ is taken as 2×2.) Combining eqns (75), (77) and (78), the energy release rate at the branched crack tip can be calculated from

$$G = \tfrac{1}{2}\tilde{\mathbf{k}}^{\mathrm{T}}\,\mathrm{Re}\,[\mathbf{Y}^0]\tilde{\mathbf{k}} \tag{79}$$

where

$$\tilde{\mathbf{k}} = \mathbf{\Theta}^{\mathrm{T}} \mathrm{Re}\,[\mathbf{t}_{\Sigma}^{\infty} * \sqrt{\cos\omega + p\sin\omega}]\sqrt{\pi a}. \tag{80}$$

These relations will be used to examine the behaviour of the energy release rate along a nearly symmetric fracture path.

The stress intensity factor result in eqn (77) has the feature that $\mathbf{k}/\sqrt{2\pi r}$ is just the asymptotic traction distribution that exists at the crack-tip along the polar plane ω before kinking. In the isotropic cases, solutions of the same feature have been proposed by Cotterell and Rice (1980) based on their first order perturbation analysis. By modelling the kinked crack as a continuous distribution of dislocations, Hayashi and Nemat-Nasser (1981) proved that the solution of Cotterell and Rice is actually correct to second order. The same conclusion can also be reached following another approach by Wu (1979a, b). Cotterell and Rice (1980) compared the second order perturbation solutions with other numerical results for cracks in isotropic solids and found that the perturbation solutions are valid over a substantial range of branch angles. For instance, agreement with the numerical results in Bilby and Cardew (1975) is within 5% up to branch angles as large as 90°.

Our analyses have extended the kinked crack solutions of Cotterell and Rice to general anisotropic cases. It is important to compare our perturbation solutions with the numerical results presented in Miller and Stock (1989) and Obata *et al.* (1989). The results of Obata *et al.* (1989) appear to be more complete than those given by Miller and Stock (1989); the latter authors also attempted to study the branched interface cracks in dissimilar anisotropic media. We choose to compare the perturbation solutions predicted by eqn (77) with the corresponding numerical results of Obata *et al.* (1989). For ease of comparison, we follow those authors in fixing the orthotropic constants as $\nu_x = -S_{xy}/S_{xx} = 0.25$ and $S_{xy} = 2(S_{xx} - S_{yy})$; the degree of anisotropy is given by the ratio S_{xx}/S_{yy} (or S_{yy}/S_{xx}).

Figures 6, 7 plot the mode I and II stress intensity factors, at different degrees of anisotropy, when the main crack lies parallel to x which is taken as the weaker material axis ($S_{xx}/S_{yy} > 1$). The perturbation results derived from eqn (77) are shown as solid lines and compared to the numerical results calculated by Obata *et al.* (1989). Amazingly, the perturbation solutions match the numerical results closely for the full range of branch angle considered by those authors, up to nearly 150°. This remarkable comparison may suggest that eqn (77) is *exact* (at least close to) for cracks with infinitesimal branches. We also use eqns (75) and (76) to calculate the energy release rate at the branched crack tip, with results shown in Fig. 8. The factor G_0 in Fig. 8 is defined in eqn (86) to follow. Our energy release rate results do not agree with those of Obata *et al.* (1989). Numerical investigation indicates that the error made by those authors lies with the compliance coefficient "c_{11}" in their eqn

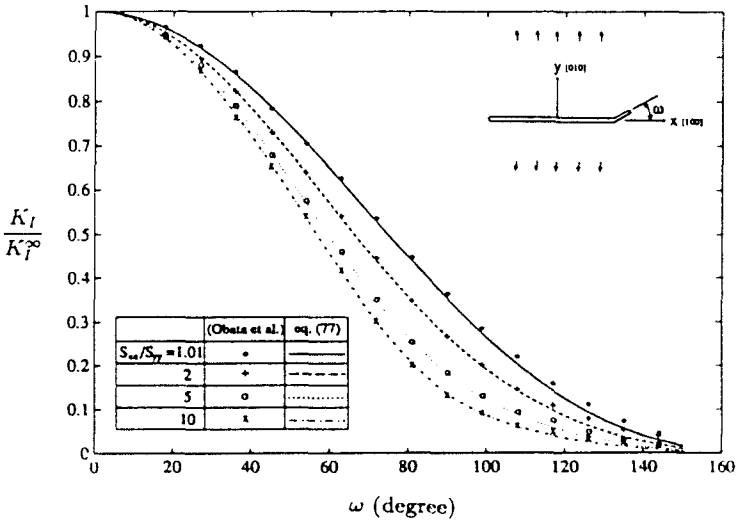

Fig. 6. The variation of mode I stress intensity factor with crack branching from a weaker material axis.

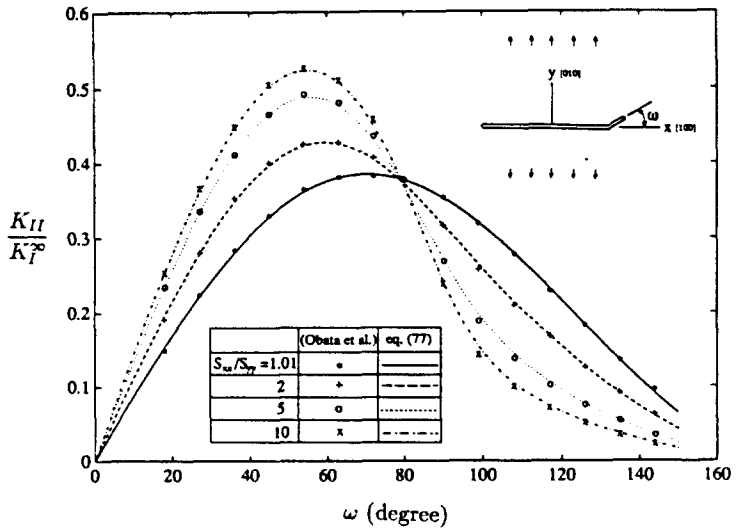

Fig. 7. The variation of mode II stress intensity factor with crack branching from a weaker material axis.

(15), corresponding to s_{11} in our notation, which should be transformed to the primed crack tip coordinates, as in our eqn (76). A major consequence of such error is that the maximum energy release rate G would appear to occur at a distinctly different branching orientation as the degree of anisotropy is increased. In contrast, our result shows that the energy release rate is always maximized at a symmetric crack orientation, regardless of the degree of anisotropy.

Figures 9 and 10 plot an asymmetric case in which the crack makes an angle of 30° with the material axis. The perturbation results for the stress intensity factors again match the corresponding numerical calculations reported by Obata *et al.* (1989) for branch angles up to nearly 150°. The energy release rate (Fig. 11) in this case is maximized at a non-zero branch angle whose magnitude increases with the degree of anisotropy.

The case when the main crack lies along the stiffer axis, i.e. $S_{xx}/S_{yy} < 1$, was not considered in Obata *et al.* (1989). Figures 12–14 plot the stress intensity factors and energy release rate in this case. Observe that, at a large degree of anisotropy, the mode I stress intensity factor becomes a local minimum with respect to branch angle. Exact transition

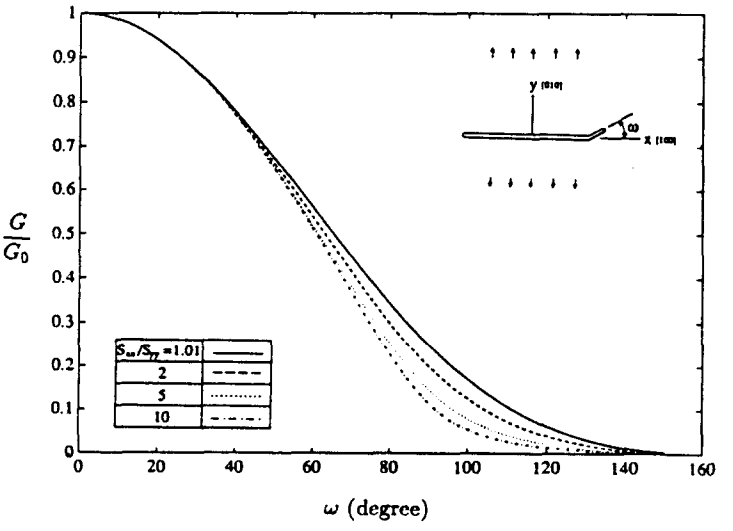

Fig. 8. The variation of energy release rate with crack branching from a weaker material axis.

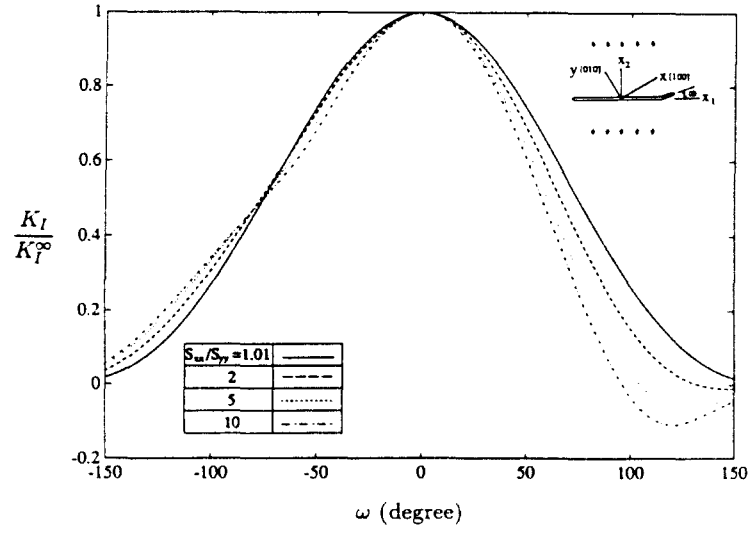

Fig. 9. The variation of mode I stress intensity factor with crack branching from an asymmetric crack orientation.

will be shown to occur when the compliance ratio $S_{yy}/S_{xx} = 4$. Obata *et al.* (1989), based on their incomplete numerical calculations for $S_{xx}/S_{yy} > 1$, concluded that the stress intensity factors have similar behaviours as the isotropic case regardless of the degree of anisotropy. Our analysis, with the inclusion of $S_{xx}/S_{yy} < 1$ cases, shows that the behaviour of stress intensity factors can change dramatically due to anisotropic effects. The crack growth criterion based on maximum K_I would predict asymmetric crack growth even under symmetric loading and material conditions, when the stiffnesses in parallel and perpendicular to the crack exceeds a four-fold ratio. Indeed, as stated by Obata *et al.* (1989), the usual crack growth criteria based on (i) maximum K_I; (ii) zero K_{II}; (iii) maximum G, which give identical predictions in the isotropic case, cease to be consistent for anisotropic solids. However, our analysis indicates that such peculiarity does not occur in the behaviour of G, as claimed by Obata *et al.* (1989), rather it is the stress intensity factors exhibiting drastically different behaviours and causing peculiar predictions under anisotropic conditions.

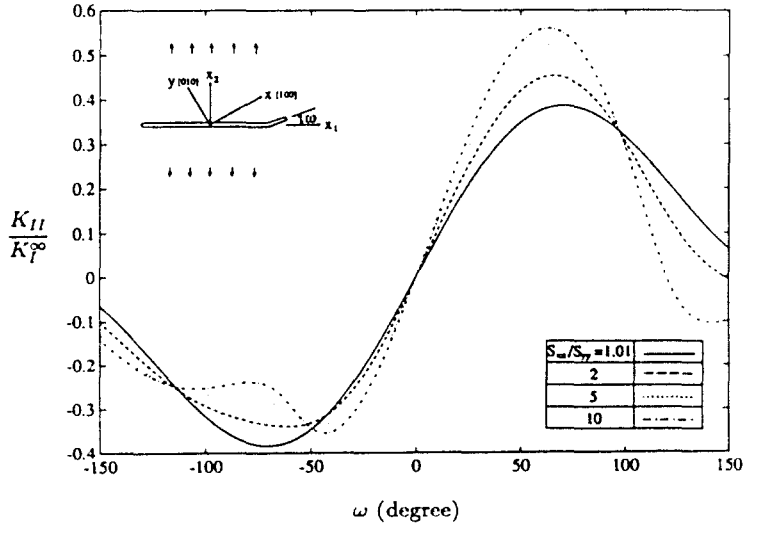

Fig. 10. The variation of mode II stress intensity factor with crack branching from an asymmetric crack orientation.

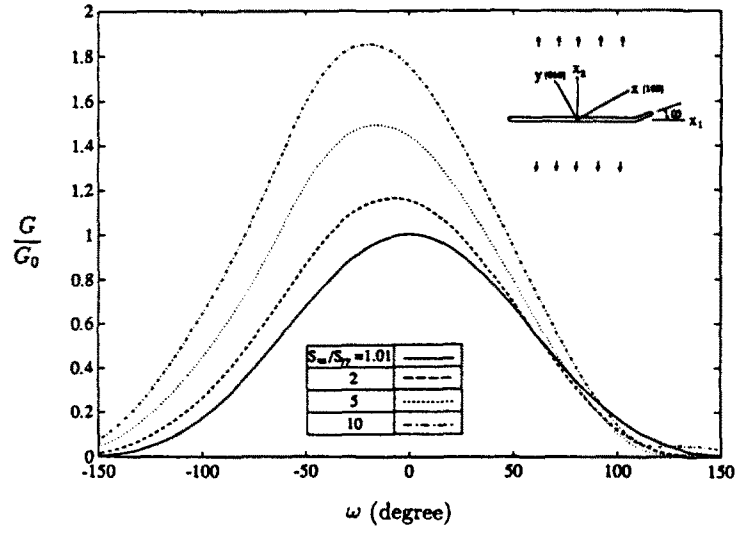

Fig. 11. The variation of energy release rate with crack branching from an asymmetric crack orientation.

Effects of mode mixity and material misorientation on crack kinking

Crack kinking occurs under asymmetric loading and/or material conditions. Thus, it is interesting to study the behaviour of cracks which are close to symmetry orientations and subjected to a slightly mixed mode loading. Figure 15 depicts our model problem for crack kinking in orthotropic solids, where the main crack lies along the x_1-axis which makes a small angle θ with the material axis x, i.e. the [100] direction. The crack is subjected to a mixed mode loading such that the apparent stress intensity factors without branching are $K_I^\infty = \sigma_{22}^\infty\sqrt{\pi a}$ and $K_{II}^\infty = \alpha K_I^\infty$. Thus, the parameter $\alpha = K_{II}^\infty/K_I^\infty = \sigma_{21}^\infty/\sigma_{22}^\infty$ denotes the mode mixity in the system.

Following eqn (77), the stress intensity factors for the above crack configuration with an infinitesimal kink that deviates by a small angle ω are given rigorously to the second order accuracy by

$$\mathbf{k} = \boldsymbol{\Omega}\,\mathrm{Re}\,[\mathbf{k}^\infty * \sqrt{\cos\omega + p\sin\omega}] \simeq \boldsymbol{\Omega}\,\mathrm{Re}\left[\mathbf{k}^\infty * \left(1 + \frac{\omega}{2}p - \frac{\omega^2}{4} - \frac{\omega^2 p^2}{8}\right)\right]. \tag{81}$$

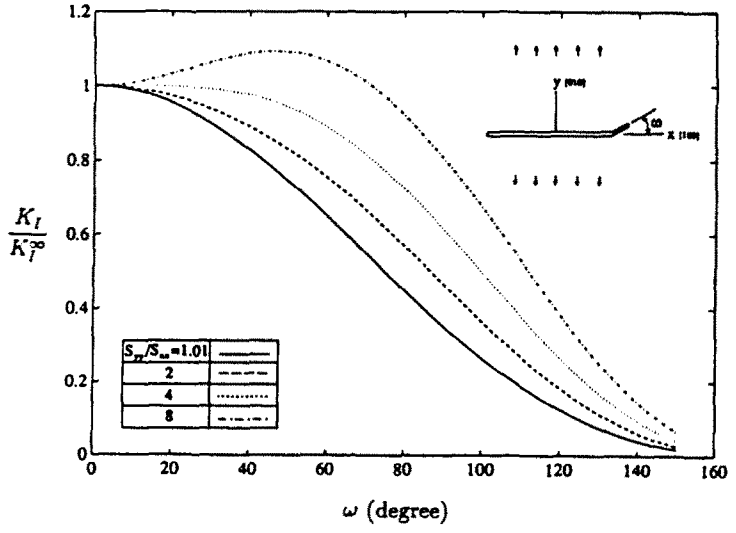

Fig. 12. The variation of mode I stress intensity factor with crack branching from a stiffer material axis.

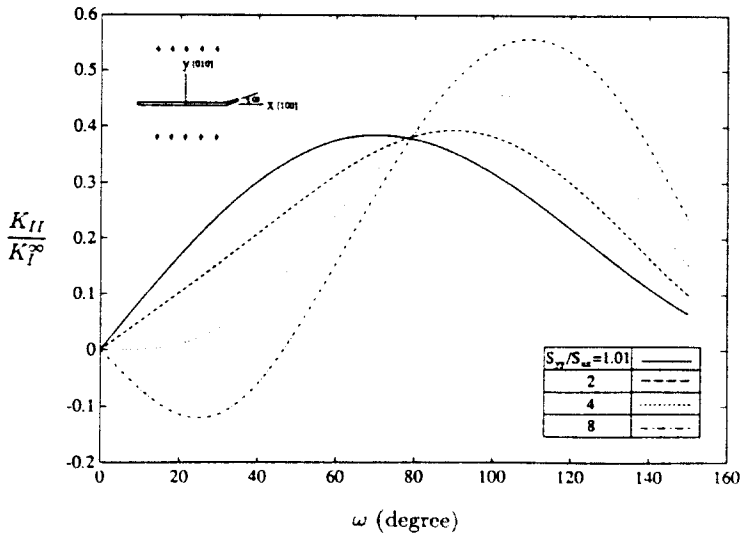

Fig. 13. The variation of mode II stress intensity factor with crack branching from a stiffer material axis.

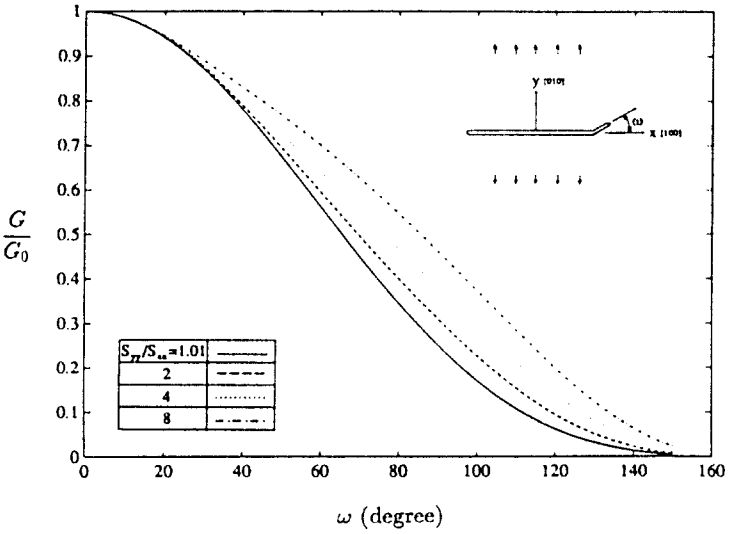

Fig. 14. The variation of energy release rate with crack branching from a stiffer material axis.

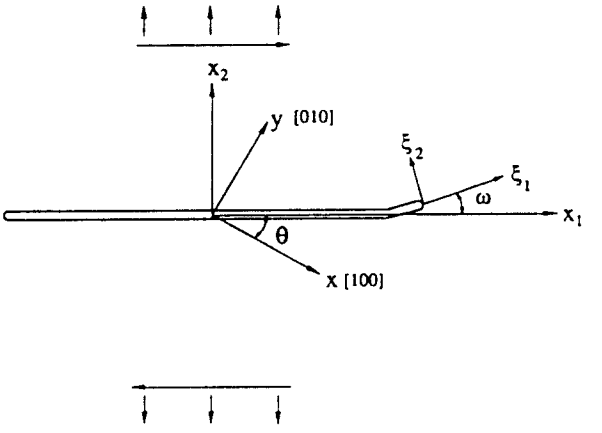

Fig. 15. A nearly symmetric crack path in orthotropic solids under slightly mixed mode loading.

The Stroh eigenvalues in the x_1 coordinates, now having angle θ with the symmetry orientation, may be obtained according to transformation in eqn (24),

$$p = \frac{p^0 \cos\theta - \sin\theta}{\cos\theta + p^0 \sin\theta} \simeq p^0(1+\theta^2) - \theta[1+(p^0)^2] \tag{82}$$

where the eigenvalues p^0 in the principal coordinates (x, y) are given in (22). Using eqns (27), (28) and (81) yields the local variation of stress intensity factors

$$K_{\mathrm{I}} = K_{\mathrm{I}}^{\infty}\left[1 - \frac{3}{4}\omega^2\left(1 - \frac{1}{2}\sqrt{\frac{S_{yy}}{S_{xx}}}\right) - \frac{3}{2}\alpha\omega\right] + 0(\varepsilon^3)$$

$$K_{\mathrm{II}} = K_{\mathrm{I}}^{\infty}\left[\alpha + \omega\left(1 - \frac{1}{2}\sqrt{\frac{S_{yy}}{S_{xx}}}\right)\right] + 0(\varepsilon^3) \tag{83}$$

for small parameters ω, θ and α. Here $0(\varepsilon^3)$ denotes quantities of at least third order, such as ω^3, $\omega^2\alpha$, $\omega^2\theta$, α^3, ... The above explicit solutions confirm an observation in Fig. 12 that, for a mode I crack lying along the stiffer material axis x with $S_{yy}/S_{xx} > 4$, the mode I stress intensity factor K_{I} becomes a local minimum with respect to the kink angle. This indicates that the conclusion of Obata *et al.* (1989), that the stress intensity factors have similar behaviours as in the isotropic case, is not true in general cases.

Some further remarks can be made concerning the behaviour of stress intensity factors:

(1) Within second order accuracy, the stress intensity factors are independent of the (off-axis) misorientation angle θ.

(2) Under mixed mode conditions, the $K_{\mathrm{II}} = 0$ crack growth criterion predicts that the crack will branch at angle

$$\omega = -\frac{2K_{\mathrm{II}}^{\infty}}{K_{\mathrm{I}}^{\infty}}\left(2 - \sqrt{\frac{S_{yy}}{S_{xx}}}\right)^{-1}. \tag{84}$$

This prediction is peculiar in that ω diverges at four-fold compliance ratio and the sign of ω reverses when $S_{yy}/S_{xx} > 4$.

(3) The maximum K_{I} criterion gives the same kinking prediction as eqn (84) when $S_{yy}/S_{xx} < 4$. When $S_{yy}/S_{xx} > 4$, K_{I} becomes a local minimum. Even under symmetric conditions, a finite branching angle is required to maximize K_{I}.

Thus, the usual K-based crack growth criteria lead to peculiar predictions whose physical significance is very questionable. For instance, there seems no reasonable justification or observation for the diverging kink behaviour at the special stiffness ratio 4. In contrast, the maximum energy release rate criterion, as will be discussed below, gives rise to no such peculiarities. These facts may simply indicate that the K-based growth criteria are not suitable for fracture analysis in anisotropic materials.

Using the stress intensity factor solution given in (83), the energy release rate G can be readily calculated from eqns (75) and (78). It is convenient to carry out the calculation using the on-axis surface admittance tensor $\mathbf{Y}^0$ given in eqn (23). The final result can be written as

$$G = G_0\left\{1 - \frac{1}{2}\left[\omega + 2\alpha - \left(1 - \sqrt{\frac{S_{yy}}{S_{xx}}}\right)\theta\right]^2 + \Lambda\right\} + 0(\varepsilon^3) \tag{85}$$

where

$$G_0 = \frac{\sqrt{S_{xx}S_{yy}}(K_I^\infty)^2}{2} \operatorname{Im}[p_1^0 + p_2^0] \tag{86}$$

$$\Lambda = \alpha^2 + \frac{1}{2}\left[2\alpha - \left(1 - \sqrt{\frac{S_{yy}}{S_{xx}}}\right)\theta\right]^2 - \left(1 - \sqrt{\frac{S_{xx}}{S_{yy}}}\right)(\alpha - \theta)^2. \tag{87}$$

Thus, when conditions at a crack tip are slightly asymmetric, the energy release rate is maximized at a small kink angle given by

$$\omega = -2\alpha + \left(1 - \sqrt{\frac{S_{yy}}{S_{xx}}}\right)\theta. \tag{88}$$

In the absence of anisotropy, i.e. $S_{xx} = S_{yy}$, this branch angle is simply $\omega = -2\alpha = -2K_{II}^\infty/K_I^\infty$, which is consistent with the corresponding isotropic result derived by Cotterell and Rice (1980) using the $K_{II} = 0$ criterion.

Assuming that the fracture resistance is uniform, the above behaviour of energy release rate leads to the following interesting observations:

(1) Loading and material asymmetries (α versus θ) play an equivalent role on crack branching near a symmetry orientation, and the effect of loading is independent of the degree of anisotropy.

(2) If the material misorientation θ is treated effectively as an additional shear mode in the system, cracks always tend to minimize the overall mode mixity by branching toward symmetric orientations.

(3) A perfectly straight and slightly off-axis crack path is possible if the effect of mode mixity just cancels that of material misorientation, namely, by imposing

$$\alpha = K_{II}^\infty/K_I^\infty = \frac{1}{2}\left(1 - \sqrt{\frac{S_{yy}}{S_{xx}}}\right)\theta. \tag{89}$$

This relation, valid when both α and θ are small, shows that one can make the crack grow along an off-axis straight path with angle θ if some prescribed shear stress is added to the system. Another implication is that when the crack is not aligned along a material symmetry orientation, there will in general not be a pure mode I fracture path. The actual path will correspond to a balance between material and loading influences.

(4) Cracks close to the stiffer material axis will behave differently from those close to the weaker axis. To see this, ignoring loading asymmetry, it can then be seen from eqn (88) that cracks tend to branch away from the weaker axis (observe that ω has the same sign as θ when $S_{yy}/S_{xx} < 1$) and branch toward the stiffer axis (ω has opposite sign to θ when $S_{yy}/S_{xx} > 1$). In other words, the anisotropy effects tend to favour the stiffer axis as the cracking orientation. This behaviour is interesting from the viewpoint that cracks in a fiber-reinforced composite material are usually expected to grow parallel to fibers. However, as pointed out by Obata *et al.* (1989), the possible anisotropic variation in the critical value of the energy release rate, G_c, should also be considered in estimating the actual growth direction.

The effect of T-stress on the stability of a symmetric crack path

Using the perturbation analysis presented above and the crack growth criterion based on maximum energy release rate, one may further address the issue of crack path stability in the sense of Cotterell and Rice (1980), who have shown that a symmetric crack path in isotropic materials is stable if the T-stress is negative and unstable if T is positive. With the understanding that the same stability issue cannot be addressed in a general sense for anisotropic materials because the fracture resistance may also be anisotropic, we shall use

Fig. 16. Crack growth behaviour influenced by non-singular T stress at the crack tip.

our perturbation results to examine the fracture path stability for those materials that do have a uniform fracture toughness value.

In the isotropic stability analysis of Cotterell and Rice (1980), the growing crack tip is assumed to be initially at the coordinate origin and subject to a slightly asymmetric loading system so that $\alpha \neq 0$. Then it was shown that, when the $K_{II} = 0$ criterion is imposed at the branched crack tip, subsequent crack growth can be approximately described as

$$A(x) = \omega_0 x\left[1 + c\frac{T}{K_I^\infty}\left(\frac{2x}{\pi}\right)^{1/2}\right] + 0(x^2) \tag{90}$$

where

$$\omega_0 = -2\alpha, \quad c = 4/3. \tag{91}$$

This growth profile tends to deflect the crack back toward the initial path if $T < 0$, and deflect the crack further away from the initial path if $T > 0$ (Fig. 16). Karihaloo *et al.* (1981) also used the $K_{II} = 0$ criterion and determined a similar crack growth profile, but with $c = 8/3$. The latter authors also pointed out that variations in K_I^∞, K_{II}^∞ due to crack tip advance† may affect the remaining terms of order x^2 in the growth profile of eqn (90).

In the anisotropic case, it does not seem proper to use the $K_{II} = 0$ criterion, as discussed before. Thus, we shall stick to arguments based on the maximum energy release rate. Consider growth by an amount l of a symmetric crack path in an orthotropic solid under a slightly mixed mode condition representing load system imperfections. This case corresponds to $\theta = 0$ and $\alpha \neq 0$. It is convenient to assume the same crack growth profile in eqn (90), with ω_0 and c to be determined from maximum energy release rate criterion. Clearly, the conclusion of Cotterell and Rice regarding the effect of T applies as long as the value of c which maximizes G is positive.

To simplify expressions in the following denote

$$v = \sqrt{S_{yy}/S_{xx}}. \tag{92}$$

Using the second order perturbation formulae (54) to calculate the stress intensity factors along the slightly perturbed fracture path (90) yields

$$\frac{K_{II}}{K_I^\infty} = \alpha + \frac{(2-v)\omega_0}{2} + \frac{T\omega_0}{K_I^\infty}\sqrt{\frac{2l}{\pi}}\left[-2 + \frac{3(2-v)c}{4}\right] - \left(\frac{T}{K_I^\infty}\right)^2\frac{3\omega_0 lc}{2} \tag{93}$$

$$\frac{K_I}{K_I^\infty} = 1 - \frac{3(2-v)\omega_0^2}{8} - \frac{3\alpha\omega_0}{2} - \frac{T\omega_0}{K_I^\infty}\sqrt{\frac{2l}{\pi}}\left[-2\omega_0 + \frac{9}{4}\alpha c + \frac{9(2-v)\omega_0 c}{8}\right]$$
$$+ \left(\frac{T}{K_I^\infty}\right)^2\frac{2l\omega_0^2}{\pi}\left[\left(6 - \frac{3\pi}{8}\right)c - \frac{27(2-v)c^2}{32}\right]. \tag{94}$$

The corresponding energy release rate G at the advancing crack tip is found to be

† Crack growth generally enlarges the overall crack size, which may result in variations of the apparent stress intensity factors.

$$G = G_0\left\{1 - \frac{1}{2}(\omega_0 + 2\alpha)^2 + \frac{1+2v}{v}\alpha^2 + \frac{T\omega_0}{K_I^c}\sqrt{\frac{2l}{\pi}}\left[-3c(\omega_0+2\alpha) + 4\left(\omega_0 - \frac{2\alpha}{v}\right)\right]\right.$$
$$\left. - \left(\frac{T}{K_I^c}\right)^2 \frac{9l\omega_0^2}{2\pi}\left[c^2 - \frac{4\pi}{3}\left(\frac{6}{\pi} - 1 - \frac{\alpha}{v\omega_0}\right)c\right]\right\} + O(l^{3/2}). \quad (95)$$

where G_0 has been given in eqn (86). Now maximizing G with respect to the parameters ω_0 and c for the lowest order term in l leads to

$$\omega_0 = -2\alpha, \quad c = \frac{2\pi}{3}\left(\frac{6}{\pi} - 1 + \frac{1}{2}\sqrt{\frac{S_{xx}}{S_{yy}}}\right). \quad (96)$$

In the isotropic case, the predicted parameter c based on the maximum energy release rate criterion is

$$c = \frac{12-\pi}{3} \simeq 2.95. \quad (97)$$

This is compared to the result $c = 4/3 \simeq 1.33$ of Cotterell and Rice and $c = 8/3 \simeq 2.67$ of Karihaloo *et al.* (1980) using the $K_{II} = 0$ criterion.

The value of c given in eqn (96) which maximizes G remains positive regardless of the degree of anisotropy, so that the conclusion of Cotterell and Rice (1980) on the crack path stability may be directly extended to the orthotropic crack problems, namely, a symmetric fracture path is stable if $T > 0$ and unstable if $T < 0$. In fact, a more heuristic argument can be used to confirm the above stability analysis. Imagine that an initially straight and symmetric crack path is subjected to a slight upward curved growth due to imperfections, so that $A'(\xi) > 0$ near the crack tip. For simplicity, let the above crack path disturbance be such that the final crack tip orientation is still parallel to the original crack. In that case, eqn (67) shows that a positive T would induce a negative K_{II}, which subsequently causes a positive branching angle $\omega > 0$ according to eqn (88) ($\alpha < 0$), so that the crack will tend to grow further away from the initial path, leading to instability. In contrast, a negative T would induce positive K_{II} and subsequently causes a negative branching $\omega < 0$ to deflect the crack back toward the initial straight path. Following this argument, it is easily seen that if the $K_{II} = 0$ criterion is used, the role of T on crack path stability would be reversed when $S_{yy}/S_{xx} > 4$ (because the branch response to a non-zero K_{II} is reversed), namely, a symmetric path becomes unstable if $T < 0$ and stable if $T > 0$, which seems contradictory to common physical intuitions.

One may also approach the stability issue from yet another perspective, which has been used by Gao (1991a) in addressing three-dimensional non-planar crack branching problems. To test the stability of a symmetric crack path, let the crack surface be subjected to an infinitesimal wavy disturbance (or, equivalently, assume that an infinitesimal fluctuation in crack surface morphology is inevitable due to imperfections). The symmetric path is then said to be stable if during subsequent growth the crack tends to propagate back toward the original position, and unstable if the subsequent growth tends to deflect the crack further away from the initial path. The kinking tendency in eqn (88) at a non-zero K_{II} suggests that the stability can be interpreted as requiring that K_{II} have a positive value at a wave peak, where the stress intensity factor solutions have been given in eqn (70) as $K_{II} = -TA\sqrt{2\pi/\lambda}$ under symmetric loading. Applying the wave-peak stability condition $K_{II} > 0$ immediately leads to the conclusion that a symmetric fracture path is stable if $T < 0$ and unstable if $T > 0$.

Under the same loading, the crack tip T-stress in an orthotropic material could be different from the corresponding isotropic solution. According to eqn (32), decreasing the stiffness in the direction perpendicular to the crack or increasing the stiffness parallel to the crack induces more compressive T stress and thus helps to stabilize the crack path. This

interesting observation is, again, consistent with the fact that cracks tend to grow parallel to fibers in unidirectional fiber-reinforced composite materials.

CONCLUSION

In this paper, we have studied a number of problems concerning slightly curved or kinked cracks in anisotropic elastic solids via a perturbation analysis valid to the second order accuracy in the deviation of the crack surfaces from a straight line. The analysis is based on complex variable representations in the Stroh formalism and known solutions for a perfectly straight reference crack. Perturbation solutions in remarkably simple forms are given in eqns (54) and (55) for the stress intensity factors at the tip of a slightly curved finite crack under remote stresses in a solid with arbitrary anisotropy. The perturbation formulae have also provided an approximate relationship in eqns (65) and (66) between the apparent and the local stress intensities at a crack tip, in view of the possible shielding effects of the crack surface morphology near the tip. We have applied the perturbation analysis to circular arc cracks, slightly jogged or kinked cracks and cosine wavy crack surface profiles, etc.

Kinking, branching and the stability of cracks in anisotropic elastic solids have been relatively less explored despite their importance. In this paper, we have attempted to address these issues in some detail. First, we have compared the predictions from the perturbation analysis with numerical results of Obata *et al.* (1989) for cracks with an infinitesimal branch length. The comparison shows that our perturbation solutions are accurate not only for small branch angles, but, amazingly, accurate for the full range of practically important branch angles, up to nearly 150°. However, our results for the energy release rate are not consistent with the corresponding results reported in Obata *et al.* (1989). We believe that the discrepancy can be attributed to an error in the energy release rate expression adopted by Obata *et al.* which has led to some false conclusions concerning the behaviour of the energy release rate with respect to crack branching in anisotropic solids. Based on our analysis, the important conclusions are:

(1) The stress intensity factors, K_I and K_{II}, can have drastically different behaviours at increasing degrees of anisotropy. The K-based crack growth criteria lead to peculiar predictions on crack branching behaviour. For instance, when the stiffness ratio parallel and perpendicular to the crack reaches four, the branch angle for mixed mode cracking based on maximum K_I or zero K_{II} criteria becomes infinite. When the same stiffness ratio exceeds four, K_I becomes a local minimum with respect to the branch angle even under symmetric conditions, as opposed to always a local maximum in the isotropic cases; in that case, the maximum K_I criterion predicts that a crack will branch away from symmetric loading orientations. These peculiar, perhaps even physically unreasonable, predictions indicate that the K-based criteria are very questionable and should not be used as the fracture criteria for anisotropic solids.

(2) In contrast to the K-based criteria, the crack growth criterion based on maximum energy release rate G, which is consistent with the K-criteria in isotropic cases, gives reasonable predictions for anisotropic cracks in all cases considered. In particular, G is always maximized locally at a symmetric crack path (as in isotropic cases). The maximum G-criterion predicts that mixed mode cracks tend to branch toward symmetric orientations. The material asymmetry about the crack plane due to anisotropy acts effectively as a loading asymmetry, the implication being that an actual crack path in anisotropic solids is in general not a "mode I" path, but one which balances the material anisotropy, loading asymmetry, and possibly also the anisotropy in fracture resistance of the material.

(3) We have also extended the analysis of Cotterell and Rice (1980) on stability of a symmetric crack path to the anisotropic cases, assuming that the fracture resistance is independent of the crack orientation. In the anisotropic case, the original approach taken by Cotterell and Rice (1980) based on $K_{II} = 0$ criterion cannot be directly applied. We show that, if maximum energy release rate criterion is used, the conclusion of Cotterell and Rice (1980) also applies to the orthotropic crack problems, namely, a symmetric fracture path

is stable if the non-singular T-stress term at the crack tip is negative and unstable if T is positive. The only difference is that the anisotropy can also influence the T-stress itself, as shown in eqn (32).

Acknowledgements—This work was supported by NSF under the Research Initiation Grant No. MSS9008521. Critical comments from two anonymous reviewers have led to substantial revision of the initial manuscript. We would like to express special thanks to each of them.

REFERENCES

Banichuk, N. V. (1970). Determination of the form of a curvilinear crack by small parameter technique. *Izv. An SSR, MTT* 7(2), 130–137 (in Russian).

Barnett, D. M. and Asaro, R. J. (1972). The fracture mechanics of slit-like cracks in anisotropic elastic media. *J. Mech. Phys. Solids* **20**, 353–366.

Barnett, D. M. and Lothe, J. (1973). Synthesis of the sextic and the integral formalism for dislocation, Green's functions and surface waves in anisotropic elastic solids. *Phys. Norv.* **7**, 13–19.

Barnett, D. M. and Lothe, J. (1974). An image force theorem for dislocations in anisotropic bicrystals. *J. Phys. F: Metal Phys.* **4**, 1618–1635.

Barnett, B. M. and Lothe, J. (1985). Free surface (Rayleigh) waves in anisotropic elastic half-spaces: the surface impedance method. *Proc. Roy. Soc. London* **A402**, 135–152.

Bilby, B. A. and Cardew, G. E. (1975). The crack with a kinked tip. *Int. J. Fract.* **11**, 708–712.

Cotterell, B. and Rice, J. R. (1980). Slightly curved or kinked cracks. *Int. J. Fract.* **16**, 155–169.

Erdogan, F. and Sih, G. C. (1963). On the crack extension in plates under plane loading and transverse shear. *J. Basic Engng* **85**, 519–527.

Eshelby, J. D., Read, W. T. and Shockley, W. (1953). Anisotropic elasticity with applications to dislocation theory. *Acta Metall.* **1**, 251–259.

Gao, H. (1991a). Three dimensional slightly non-planar cracks. *J. Appl. Mech.* (in press).

Gao, H. (1991b). Morphological instabilities along surfaces of anisotropic elastic solids. In *Modern Theory of Anisotropic Elasticity and Applications* (Edited by J. C. Wu, T. C. T. Ting and D. M. Barnett). SIAM, Philadelphia (in press).

Gao, H., Abuddi, M. and Barnett, D. M. (1991). On interfacial crack-tip field in anisotropic elastic solids. *J. Mech. Phys. Solids* (in press).

Goldstein, R. V. and Salganik, R. L. (1970). Plane problems of curvillinear cracks in an elastic solid. *Izv. An SSR, MTT* 7(3), 69–82 (in Russian).

Goldstein, R. V. and Salganik, R. L. (1974). Brittle fracture of solids with arbitrary cracks. *Int. J. Fract.* **10**, 507–523.

Hayashi, K. and Nemat-Nasser, S. (1981). Energy-release rate and crack kinking. *Int. J. Solids Structures* **17**, 107–114.

He, M.-Y. and Hutchinson, J. W. (1989). Kinking of a cracks out of an interface. *J. Appl. Mech.* **56**, 270–278.

Hussain, M. A., Pu, S. L. and Underwood, J. (1974). Strain energy release rate for a crack under combined mode I and mode II. *ASTM STP* **560**, 2–28.

Ingebrigtsen, K. A. and Tonning, A. (1969). Elastic surface waves in crystals. *Phys. Rev.* **184**, 942–951.

Karihaloo, B. L., Keer, L. M., Nemat-Nasser, S. and Oranratnachai, A. (1981). Approximate description of crack kinking and curving. *J. Appl. Mech.* **48**, 515–519.

Lekhnitskii, S. G. (1963). *Theory of Elasticity of an Anisotropic Elastic Body* (translated by P. Fern). Holden-Day, San Francisco.

Lo, K. K. (1978). Analysis of branched cracks. *J. Appl. Mech.* **45**, 797–802.

Miller, G. R. and Stock, W. L. (1989). Analysis of branched interface cracks between dissimilar anisotropic media. *J. Appl. Mech.* **56**, 844–849.

Obata, M., Nemat-Nasser, S. and Goto, Y. (1989). Branched cracks in anisotropic elastic solids. *J. Appl. Mech.* **56**, 858–864.

Palaniswamy, K. and Knauss, W. G. (1978). On the problem of crack extension in brittle solids under general loading. In *Mechanics Today* (Edited by S. Nemat-Nasser). Pergamon Press, Oxford.

Savin, G. N. (1961). *Stress Concentration around Holes*. Pergamon Press, Oxford.

Sih, G. C. (1973). A special theory of crack propagation. In *Mechanics of Fracture* (Edited by G. C. Sih). Noordhoff, Leyden.

Sih, G. C., Paris, P. C. and Irwin, G. R. (1965). On cracks in rectilinearly anisotropic bodies. *Int. J. Fract. Mech.* **1**, 189–203.

Stroh, A. N. (1958). Dislocations and cracks in anistropic elasticity. *Phil. Mag.* **7**, 625–646.

Stroh, A. N. (1962). Steady state problems in anisotropic elasticity. *J. Math. Phys.* **41**, 77–103.

Sumi, Y. (1986). A note on the first order perturbation solution of a straight crack with slightly branched and curved extension under a general geometric and loading condition. *Engng Fract. Mech.* **24**, 479–481.

Sumi, Y., Nemat-Nasser, S. and Keer, L. M. (1983). On crack branching and curving in a finite body. *Int. J. Fract.* **21**, 67–79.

Suo, Z. (1990). Singularities, interfaces and cracks in dissimilar anisotropic media. *Proc. Roy. Soc. London* **A427**, 331–358.

Ting, T. C. T. (1982). Effects of change of reference coordinates on the stress analyses of anisotropic elastic materials. *Int. J. Solids Structures* **20**, 139–152.

Tsai, S. W. and Hahn, H. T. (1980). *Introduction to Composite Materials*. Technomic Publishing Company, Lancaster, Pennsylvania.

Wu, C. H. (1979a). Fracture under combined loads by maximum-energy-release rate criterion. *J. Appl. Mech.* **46**, 553–558.

Wu, C. H. (1979b). Explicit asymptotic solution for the maximum energy-release rate problem. *Int. J. Solids Structures* **15**, 561–566.